HiSST: International Conference on
High-Speed Vehicle Science Technology
26–29 November 2018, Moscow, Russia

EFFECT OF ROUGHNESS OF BLUNTNESS NOSE ON THE LAMINAR-TURBULENT TRANSITION AT HIGH MACH NUMBERS

P.A. Polivanov[1], Yu.V. Gromyko[1], D.A. Bountin[1], A.A. Maslov[1]

Abstract

Laminar-turbulent transition on the blunt leading edge generated by roughness can lead to a sharp growth of heat fluxes on the surface of hypersonic vehicles. Experimental study of the roughness was performed in the T-327b and "Transit - M" wind tunnels on a conical model at two Mach numbers M = 5, 6 at wide range of the Reynolds number Re_1 = 3-68·10^6 1/m and radius of bluntness R=2-9 mm. Three types of roughness were considered: distributed, isolated, and combination of two single roughness. Nonstationary measurements of pressure pulsations on the model surface, mass flow rate and measurement of heat fluxes were performed. In the study the effect of roughness on the turbulization of the boundary layer dependence on Reynolds number was found. The effect of the roughness geometry on the laminar-turbulent transition was studied. Data analysis showed the main features of the flow around the roughness.

Keywords: *laminar-turbulent transition, roughness, hypersonic.*

Introduction

Wall roughness can exert a significant effect of the heat flux distribution on hypersonic flying vehicles, which is mainly caused by shifting of the laminar-turbulent transition region. High thermal loads can induce changes the wall roughness elements during the flight owing to ablation of the thermal protection material, surface erosion, etc. The appearance of random roughness on nose part has a high probability because usually in this region there is a maximum of thermal loads. For the design of the thermal protection system for hypersonic vehicles requires reliable criteria of estimating the influence of roughness on the laminar-turbulent transition along the entire trajectory [1, 2]. In most studies investigating this problem are considered variants of distributed [3] or a single [4] roughness. The local Mach number can have a significant effect on the development of perturbations downstream the roughness [1]. But most of the papers were carried out for boundary layers without a pressure gradient or with a slight change of the flow parameters along streamwise near the roughness. On the blunt leading edge with a small diameter there is observed an acceleration of the flow, which can significantly effect on the roughness turbulization. In this study it was decided to find Reynolds numbers at which the boundary layer behind the roughness placed on bluntness nose became turbulent.

The characteristic height of the roughness is included in all the empirical criteria used to determine the onset of flow turbulization. In contrast to the single roughness for the case of distributed roughness there are many options for calculating this height. The lack of understanding of the physical processes of the development of disturbances generated by the distributed roughness does not allow to uniquely determine the way transition mechanism. To improve understanding of the processes of interaction of roughness wake for case a distributed roughness, it was decided to investigate the simplified case. For this purpose a study of the turbulization of the boundary layer behind two single roughness located close to each other was performed.

[1] *Khristianovich Institute of Theoretical and Applied Mechanics SB RAS 630090, Institutskaya, 4/1, Novosibirsk, Russia, polivanov@itam.nsc.ru*

1. Experimental setup

The experimental study was divided into two parts. The location of the laminar-turbulent transition was determined in the short-duration "Transit-M" wind tunnel [5] with wide range of Reynolds numbers. But in this wind tunnel only surface measurements on the model can be performed. It is make difficult to analyze the flow near roughness. Additional experiments were performed in the T-327b wind tunnel, where the run duration allowed to investigate the flow near the roughness by hot-wire anemometer.

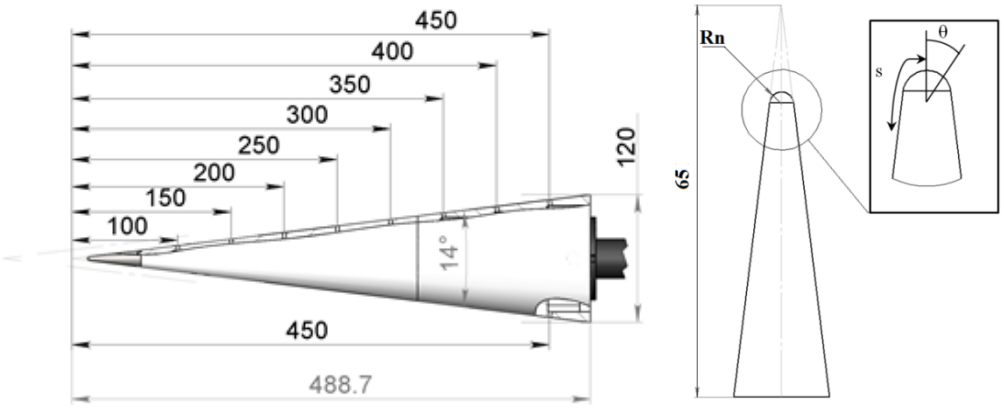

a b

Fig 1. Schematic representation of the model with the location of the surface pressure sensors (a) and an enlarged model nose with the designation of the coordinate x and the roughness angle Θ (b). Dimensions are in millimeters.

The experiments were carried out in the hypersonic wind tunnel "Transit-M" of ITAM SB RAS at the Mach number 5.95, the stagnation temperature T_0 = 361 ÷ 421 K and the deceleration pressure P_0 = 3.5 – 46 atm. The unit Reynolds number varied in the range Re_1 = (4.2 ÷ 69.7)×10^6 m^{-1}. The diameter of the outlet section of the nozzle was 300 mm, air was used as the working gas.

Investigation of the influence of roughness on the laminar-turbulent transition of the boundary layer was carried out on a cone model with half-angle of 7° with interchangeable noses. The model was made from plastic (polyacetal) to perform thermal field measurements with IR-camera, and was equipped with high-frequency surface pressure sensors PCB 132A31 (see Fig. 1a). A total of 8 pressure sensors were installed along the generating line of the cone, and the 9th sensor was located symmetrically to the eighth on the opposite side to control the angle of attack. The model was installed in the working section at zero angle of attack, along the axis of the nozzle and was partially recessed into it. The distance from the trailing edge of the model to the section of the nozzle was 325 mm.

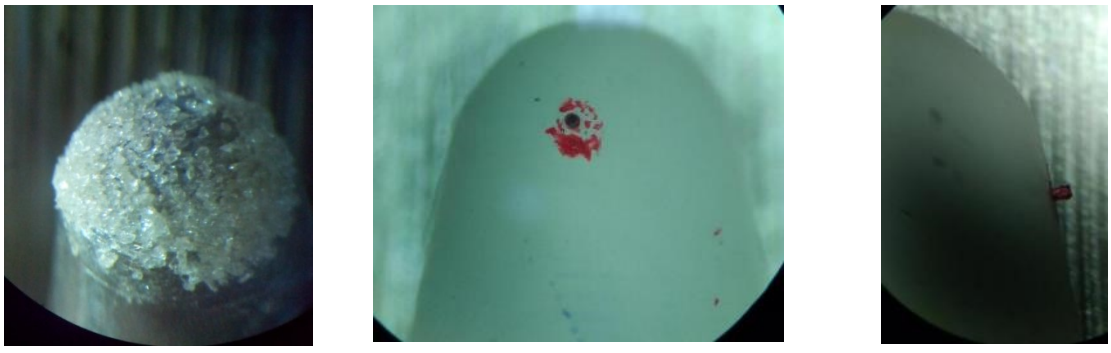

a b c

Fig 2. Noses with roughness: a - distributed roughness; b - single roughness Rn = 2 mm, k = 100 μm; c - single roughness Rn = 5 mm, k = 480 μm.

The experiments were performed for two types of roughness: distributed (see Fig. 2a) and isolated (see Fig. 2b, c). The distributed roughness (roughness height $Ra \approx 28$ and 60 μm for $Rn = 2$ and 5 mm, which is defined as the standard deviation of surface depressions or bulges from the center line of the surface) was made using two types of calibrated sand, pasted onto a nose, sand was applied at an angle $\Theta = 90$ °, and then, as necessary, it was cleaned to the desired angle Θ (see Fig. 1b). As a material for the production of an isolated roughness, a line was chosen which allowed to accurately control the diameter of the roughness with high accuracy.

Measurements of temperature fields on the surface of the model were performed using a Flir sc7000 thermal imager with a 7300M matrix consisting of 320 × 256 elements. The spectral range of the device is 3.7 ÷ 4.8 μm, the temperature range of measurements is 5 ÷ 150 ° C. The frame rate in the experiments was 300 Hz. During the start-up time, the surface of the model was heated by 1 to 2 degrees. To find the magnitude of the unsteady heat flux, the Cook-Felderman algorithm [6] was applied, which makes it possible to obtain a solution to the problem of heat propagation in a semi-infinite body.

Pressure sensors were used in conjunction with the signal converter PCB Piezotronocs 482C05. Data collection from PCB sensors was performed by three four-channel L-card E20-10 ADCs synchronized with the control system with a frequency of up to 1.7 MHz. The power spectra were calculated on the basis of a discrete Fourier transform. The spectral distributions were calculated by averaging over L blocks of 2^N points in each block in time diapason of run 95 ÷ 10 ms. The number of blocks was 65, with the number of points in block 256.

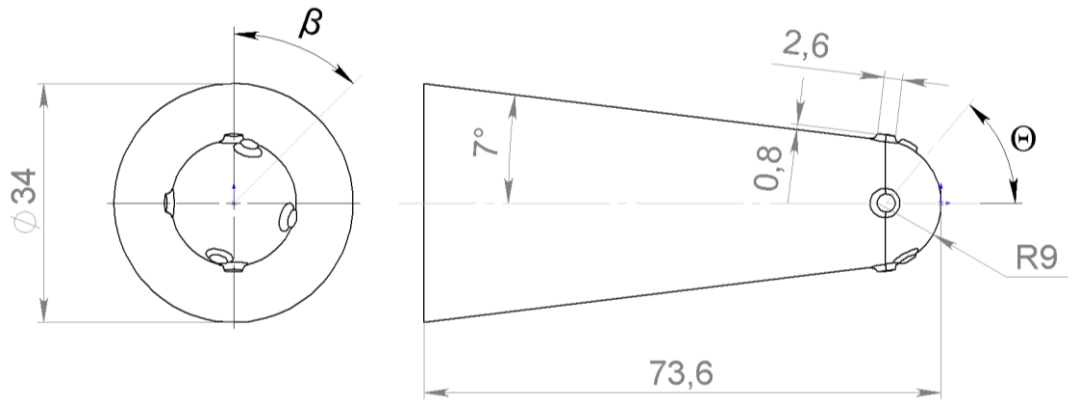

Fig 3. Example of a model drawing studied for the wind tunnel T-327b

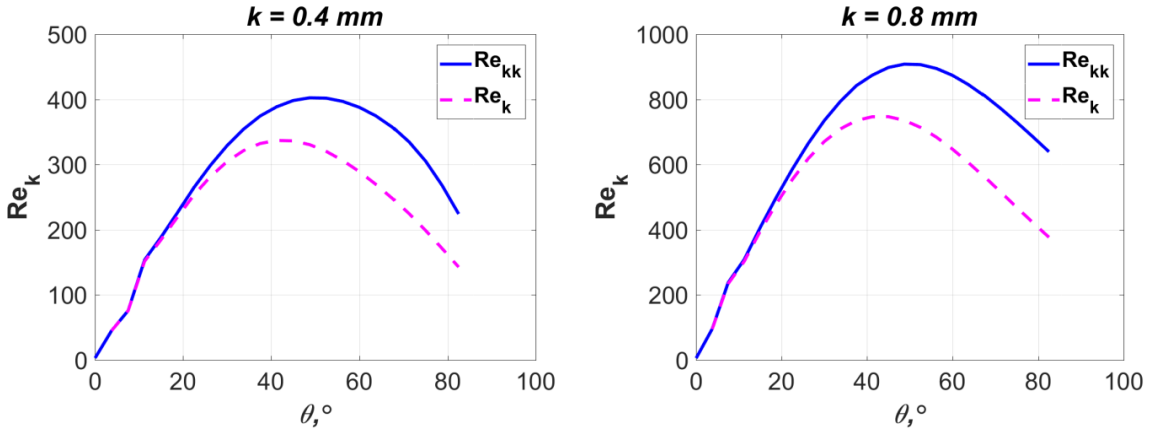

Fig 4. The distribution of the Re_{kk} and Re_k along the nose part of the model for different roughness heights

The experiments of determining flow around elements of roughness were carried out in the T-327b ITAM SB RAS wind tunnel [4]. The run duration of this wind tunnel is approximately 35-55 s. The present experiments were performed at the Mach number M = 5, stagnation temperature T0 = 295 K, stagnation pressure $P_0 = 100$ kPa, and unit Reynolds number $Re_1 = 3.2 \cdot 10^6$ m_{-1}. Four experimental

blunted cone models with a half-angle 7°· were developed and manufactured. On each model there were 4 types of roughness. Two of them were single, and the remaining two were their combination. This made it possible to investigate the effect of interference of waves behind two roughnesses on laminar-turbulent transition. In this paper several mutual arrangement of two roughnesses and their geometries were studied. An example of a model drawing is shown in Fig. 3. In figure can be seen four groups of roughness spaced by β=90° degrees. Two cases corresponded to single roughnesses located at Θ = 63 and 83°· at a height of 0.8 mm. The other two cases are a combination of two roughnesses located approximately at 45° (the angle between the plane of symmetry and the line drawn through the centers of roughness). On other experimental models other heights of and relative locations of roughnesses were investigated. The shape of the roughness was a cylinder with a fillet (r = 0.5 mm) along the line of between roughness and the model (the fillet appeared due to the characteristics of the tool used on the CNC machine). The main measurements were carried out by a constant temperature anemometer. Additional data about the flow pattern were obtained by the PIV method and the infrared camera.

The height of the roughness was chosen on the basis of previous studies carried out for a single roughness [4] and the Reynolds number based on the height of roughness. In the study of roughness, two ways of calculating the Reynolds number are widely used [7, 8], which have differences in the viscosity used in the equation:

1) $$\mathrm{Re}_{kk} = \frac{\rho_k U_k k}{\mu_k} \quad (1);$$

2) $$\mathrm{Re}_{k} = \frac{\rho_k U_k k}{\mu_w} \quad (2).$$

Where k is the height of the roughness, ρ_k and U_k – the density and velocity at the roughness height, μ_w and μ_k are the viscosity on the wall and at the roughness height.

It has been found empirically [1,2,8] that at a Re_{kk} > 450 the boundary layer turbulization arises immediately after the roughness. Figure 4 shows the distribution of Re_{kk} and Re_{k} along the blunt nose of model. For a roughness height of k = 0.4 mm the value Re = 450 is not achieved in the all range of Θ for both ways of calculating the Reynolds number. An increase the height to k = 0.8 mm results in exceeding the edge Re = 450 for both methods of calculating the Reynolds number for angles Θ = 63 and 83° (roughness locations). This means that for a case with single roughness at k = 0.4 mm, turbulence should not arise after single roughness and for the case k = 0.8 mm turbulization of boundary layer will immediately be behind the roughness. The previous experimental results [4] confirmed the correctness of this relation.

In this paper the effect of a combination of two roughnesses on the turbulization process was study at roughness heights at which Re_{kk} < 450. In addition a features of the turbulent wake generated by two roughnesses with Re_{kk} > 450 was considered.

2. Experimental results

2.1. Distrivuted roughness

An experimental study was carried out for all types of roughness. Effective values of Reynolds numbers were obtained at which the laminar-turbulent transition occurs on the model's nose. In Fig. 5 is shown a graph of the effective unit Reynolds numbers multiplied by the Ra values for different angles of deposition of the distributed roughness. For both radii of blunting, it is clear that when the angle of roughness increases, the effective Reynolds number decreases, until the angle reaches 90°. This indicates that for all the investigated radii of blunting and roughness, the minimum unit Reynolds number at which the laminar-turbulent transition occurred on the model nose corresponds to the angle Θ = 90°. This result was unexpected. According to the computational study, the most critical location of the roughness is near the sonic line ($\Theta \approx 45°$) in which Re_{kk} acquires the maximum value, i.e. with the angle Reef should be minimal. However, as can be seen from the experimental data, Re_{ef} becomes minimal at Θ = 90 °.

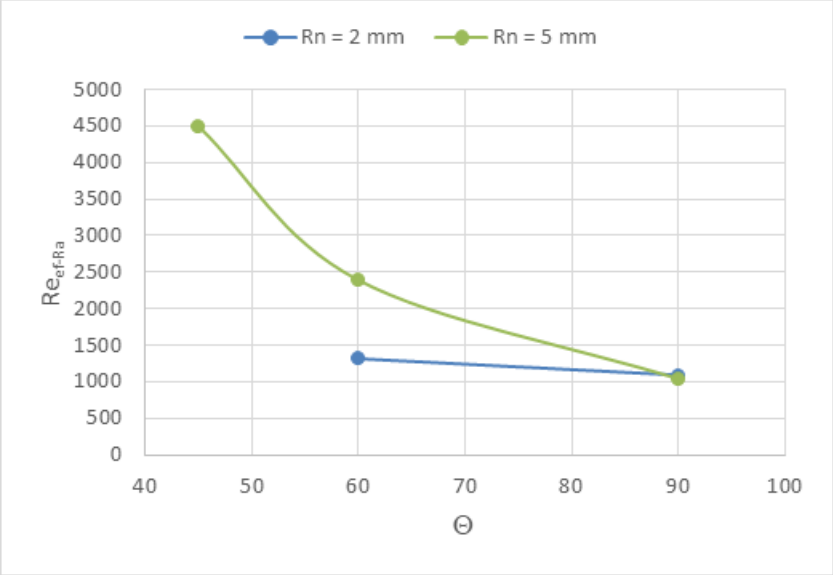

Fig 5. Unit Reynolds number, at which a laminar-turbulent transition occurred on the nose, multiplied by the average roughness height ($Re_{efRa} = Re_1 \cdot Ra$) dependence on application angle of the roughness Θ.

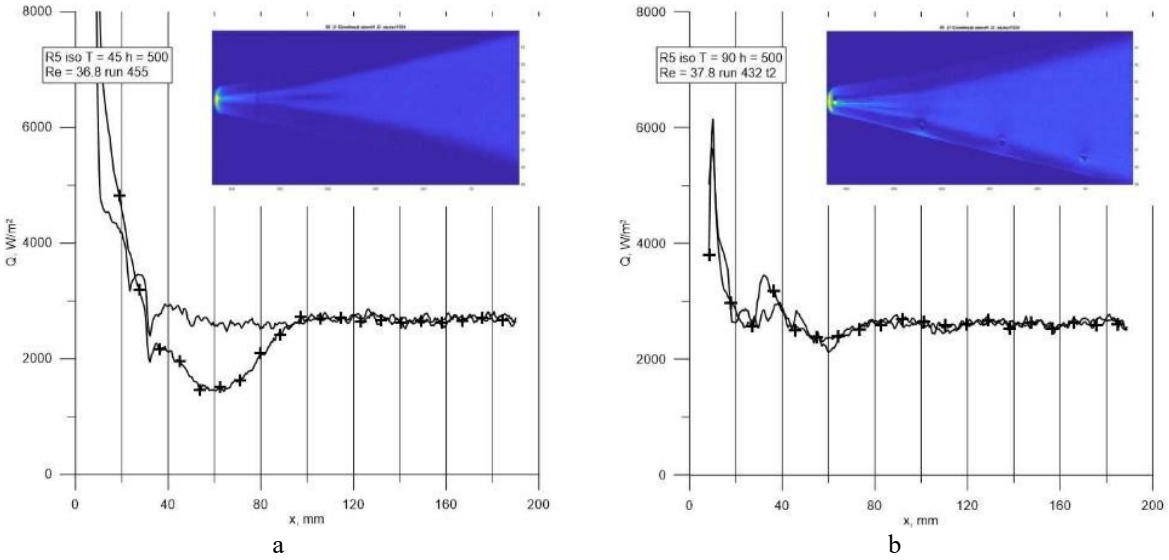

Fig 6. Distribution of heat fluxes behind the wake of a single roughness for R = 5 mm, k = 600(a) and 480(b) μm, d=300 μm. a - $Re_1=36.8 \cdot 10^6$ 1/m, Θ=45°; b - $Re_1=37.8 \cdot 10^6$ 1/m, Θ=90°.

2.2. Isolated roughness

In Fig. 6 shows the difference in the thermal trace for angles Θ = 45° and 90° for a isolated roughness of height k = 500 μm on the nose Rn = 5 mm measured in "Transit - M". The line with crosses corresponds to the center line behind the roughness, the line without the symbols corresponds to the ray with the maximum heat flux. In all cases, the laminar-turbulent transition occurred immediately after the roughness. That is understandably from the absence of a minimum along the ray with the maximum heat flux (line without symbols, range X = 30 - 100 mm). In the case Θ = 45° heat fluxes is decreased along the central ray, where local minimum clearly saw (range X = 30 - 100 mm, line with crosses). Probably, two vortices of turbulent wakes are formed from roughness and afterwards form two turbulent wedges that merge downstream. The figure of Θ = 90° has some difference: after the roughness the wedge with of increased heat flux is attended and two side wakes, similar to the picture at Θ = 45° is clearly visible. At the same time, along the central

line, a local minimum of the distribution of heat flux is preserved, although it is weakly expressed. This behavior is maintained for all types and angles of a single roughness.

2.3. The influence of roughness on the development of disturbances.

For each run, the spectra of surface pressure pulsations of the models were obtained by PCB sensors. Examples of spectra for sensors in X = 100mm and X = 250mm are shown in Fig. 7. Amplitude spectra, normalized on the presure of border of the boundary layer for distributed roughness with the angle of application Θ = 90º, 60º, 45º, single roughness, standing at Θ = 45º and smooth nose (Rn = 5 mm) is presented.

In the case of a single roughness, the pressure sensors were oriented, thus, to be on the same line as the roughness, in order to trace the pulsations in the vortex wake.

The first sensor (X = 100 mm, Fig. 7a) shows that for a roughness with an angle of application Θ = 90º, the pulsation spectrum is completely filled, which indicates the end of the laminar-turbulent transition in front of the sensor. For a roughness with an angle of application of Θ = 60º, an increase in pulsations is observed between the first sensor (Fig. 7a), which indicates the commencement of intermittency, which downstream grow to end laminar-turbulent transition. For cases of distributed and single roughness with Θ = 45º, the pulsation spectra are characteristic for a laminar boundary layer. At X = 250 (Fig. 7b), the spectrum for Θ = 45° for almost filled, which indicates the imminent end of the laminar-turbulent transition. Downstream, the boundary layer is turbulent for all roughness cases. It is important to note that for a smooth spout the level of pulsations corresponds to a laminar boundary layer, but the roughness leads to an increase in the perturbations compared to a smooth spout, with no identified frequencies in the spectra behind the roughness observed (means about perturbations associated with the second mode of Mack). And the effect is enhanced, with an increase in the area of application of roughness.

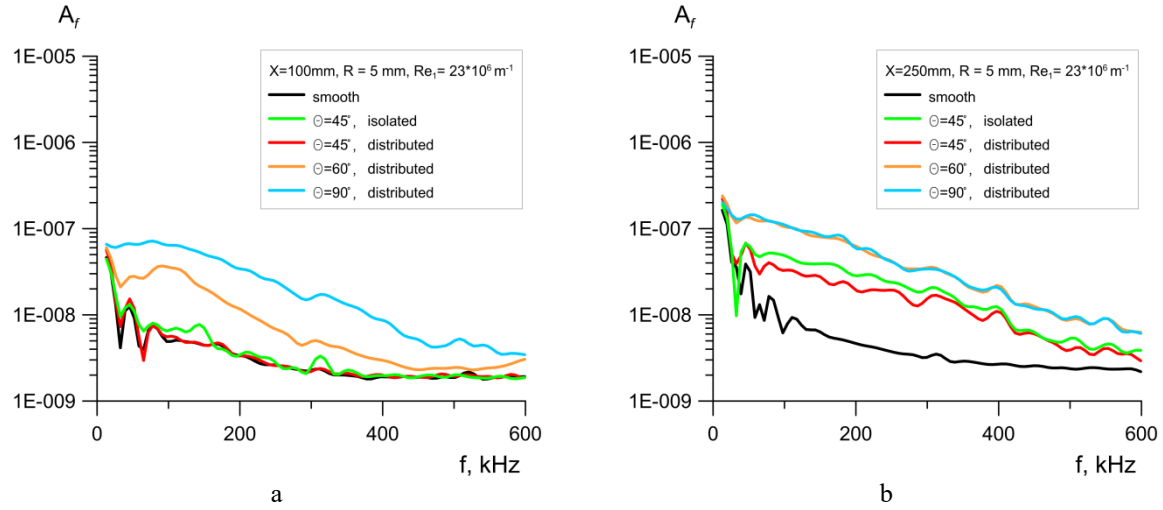

Fig 7. Distribution of pressure pulsation spectra on the wall, Rn = 5 mm, Re_1 =23·10^6 1/m.

2.4. The study of the deformation profiles of mass flow rate in the wind tunnel T-327b

Figure 8 shows the mass flow rate distribution along the azimuthal coordinate β for various combinations of heights of roughnesses measured by a hot-wire anemometer. The value β = 0º corresponds to the roughness element position for case Θ = 63º. The plane of symmetry for roughness at Θ = 83º is located at β ≈ 20º. In the figures a defect of the velocity distribution behind single roughness is clearly visible. For case Θ = 63º the fullness of the boundary layer is significantly higher than for case Θ = 83º. This is explained by the larger Re_{kk} value for the roughness Θ = 63º (Figure 4). But for both case the profile of the boundary layer does not correspond to the developed turbulent flow. Cases with two roughnesses increase the deformation and fullness of the profile as compared to cases of single roughness.

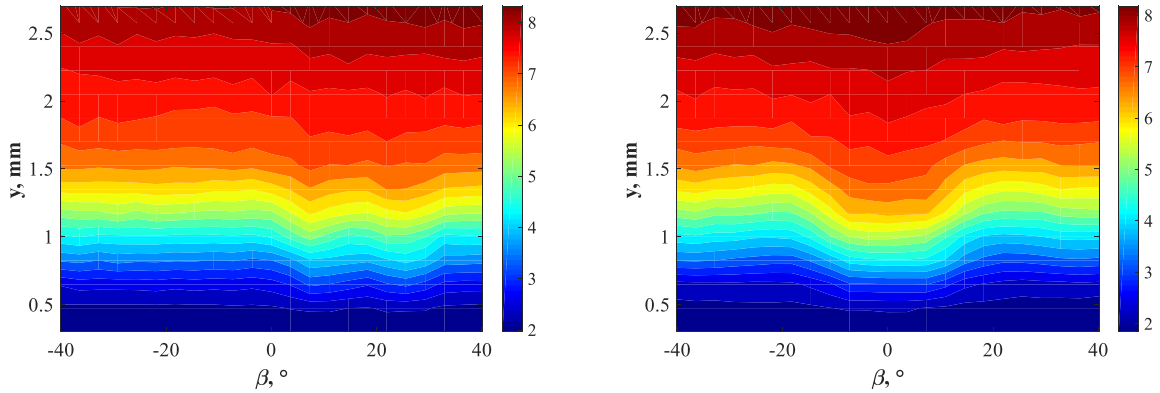

Θ = 83°, k = 0.4 mm

Θ = 63°, k = 0.4 mm

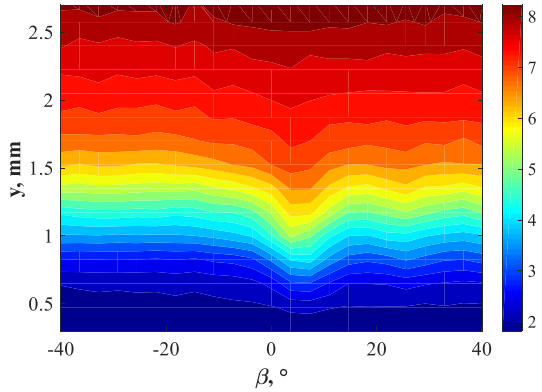

Θ = 63°, k = 0.2 mm; Θ = 83°, k = 0.4 mm

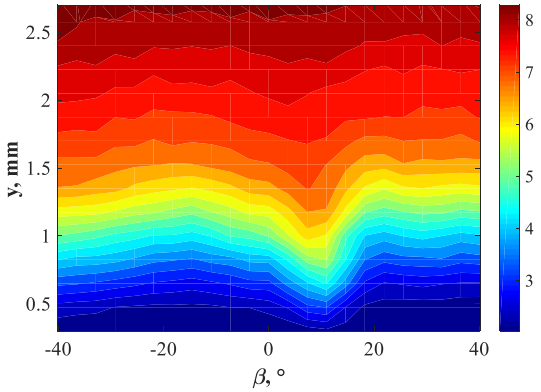

Θ = 63°, k = 0.4 mm; Θ = 83°, k = 0.4 mm

Fig 8. Distribution of mass flow rate [kg/(m2·s)] in section X = 52 mm for different heights of roughness

The data measured at a distance of 52 mm from the nose of model for two models is shown in Fig. 9. The heights of the investigated roughnesses are in the legend of the figure. The lines on Fig. 9a,c are constructed on the basis of points where the mass flow rate was 75% of the mass flow rate on the interface between the main flow and the boundary layer. The asymmetry coefficient along the isoline is shown in Fig. 9b,d. The profile of the boundary layer behind single roughnesses with height k = 0.8 mm corresponds to the turbulent boundary layer (Fig. 9a). This is confirmed by PIV measurements. The combination of roughnesses still generates a turbulent flow in the wake, but a significant modification of the flow is clearly visible. For example a "small" roughness with k = 0.4 mm at Θ = 63° added before a "large" roughness with k = 0.8 mm at Θ = 83° shifts the zone with a large fullness of profile (turbulent region) to the wake of "small" roughness. It is interesting to note that the boundary layer behind the "large" roughness (Θ = 83°) becomes closer to the laminar. An increase in the roughness height of the located Θ = 63° from k = 0.4 to k = 0.8 mm leads to an expansion of the turbulent zone in the direction of the roughness case Θ = 83°. It can be assumed that the reason for this is the interference of vortices formed around the roughness, which for this configuration leads to a significant increase in the disturbances developing between the roughnesses and weakening of others. This conclusion confirms the visualization of wall temperature by infrared camera. From the asymmetry distribution (Figure 9b) it can be seen that the interference of the wake behind the roughness leads to a significant deviation of the asymmetry from the normal distributional at the center of the zone of turbulence. This is significantly different from the case of a single roughness which the deviation of the coefficient of asymmetry from zero is found at the side edge of the turbulent wedge.

Reduce by half the height of the roughness (Fig. 9c,d). It is clearly seen that for the case of two roughnesses shows an increase in deformation in the distribution of mass flow rate in the wake (Fig. 9c, β = 9°) at comparison with a single case. This flow pattern is similar case with a doubled height of roughness described above. This can be explained by the large "effective" diameter of the doubled roughness. But although the fullness of the profile increases, the region of the turbulent flow

narrows in comparison with the case of a single roughness (Fig. 8 and Fig. 9c) which is similar to Fig9a. Therefore it can be assumed that the process of interference of roughness wake depends weakly on their hight. And the cause of increased turbulence at small k = 0.4 mm is the union of the vortices. For the case of a interfering roughnesses coefficient of asymmetry in the turbulent region becomes significantly negative, which means that there is a non-equilibrium turbulent boundary layer in this region.

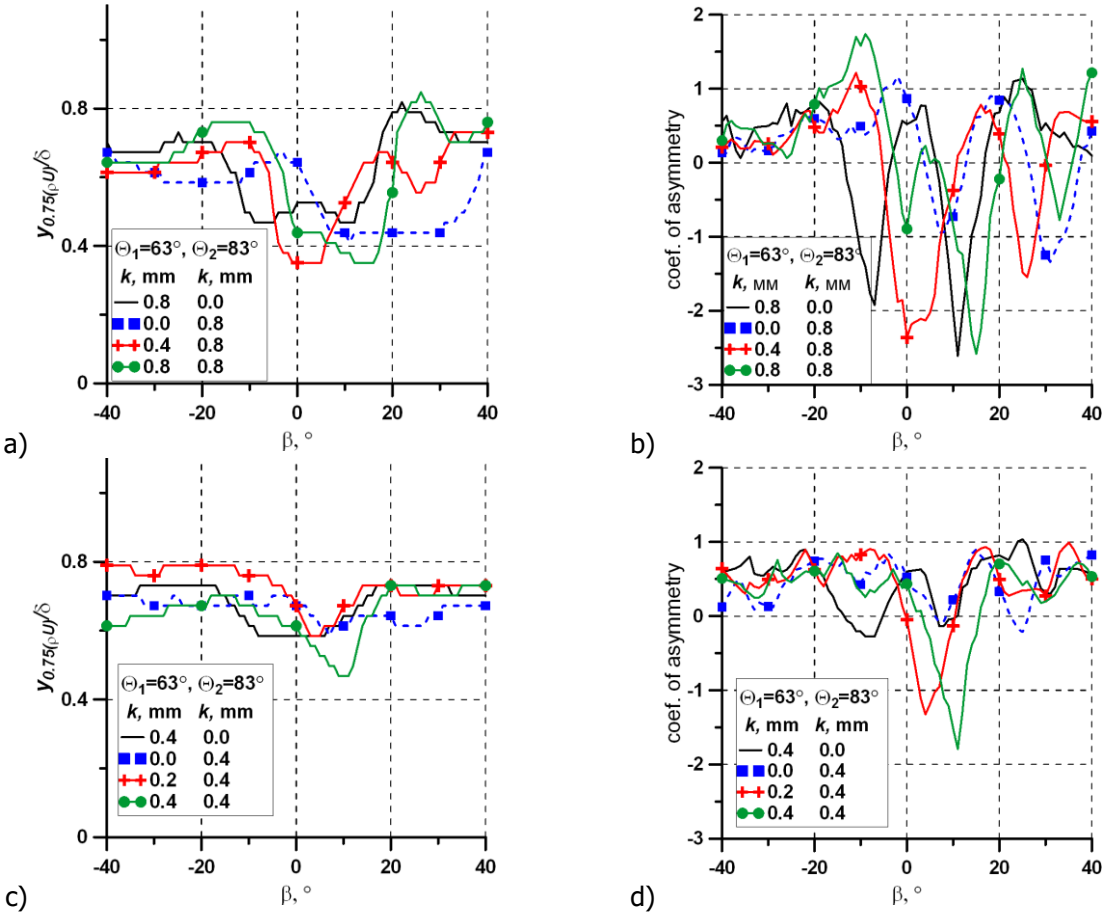

Fig 9. Flow rate isoline (a,c) and coefficient of asymmetry (b,d) in section X = 52 mm.

Conclusion

Experiments with distributed roughness showed that the most critical location of the roughness is near the conjugation line of the spherical part and the cone ($\Theta \approx 90°$): the unit Reynolds number at which the transition occurs immediately after the roughness is minimal. It was also shown that the presence of a roughness significantly influences the growth of perturbations in the boundary layer, and can lead to an earlier turbulence of the flow.

It is confirmed that the Reynolds number Re_{kk} is a reliable criterion for determining the turbulization of the boundary flow behind a single roughness. It was found that for the case of two roughnesses the turbulization of the boundary layer can be more intense and accordingly the value of the Re_{kk} criterion can decrease.It was found that two roughnesses case can lead to increased turbulence and accordingly a decrease the value of the empirical criterion of Rekk. On the basis of the data analysis it was suggested that the main reason for the change in the turbulization of the boundary layer behind two roughnesses is the interaction of the vortices generated by the roughnesses.

Acknowledgments

The work was supported by grant of RSF 14-11-00490-p, PIV measurement were performed during the project supported by grant RFBR 18-01-00536a.

References

1. S.P. Schneider: Effects of Roughness on Hypersonic Boundary-Layer Transition. J. Spacecraft and Rockets. 45, 193–209 (2008).
2. S.P. Schneider: Summary of Hypersonic Boundary-Layer Transition Experiments on Blunt Bodies with Roughness. J. Spacecraft and Rockets. 45, 1090-1105 (2008).
3. Bountin D.A., Gromyko Yu.V., Maslov A.A., Polivanov P.A., Sidorenko A.A.: Effect of the surface roughness of blunt cone forebody on the position of laminar-turbulent transition. Thermophysics and Aeromechanics. 23, 629–638 (2016).
4. Polivanov P.A., Gromyko Yu.V., Sidorenko A.A., Maslov A.A. Turbulization of the wake behind a single roughness element on a blunted body at a hypersonic Mach number. Journal of Applied Mechanics and Technical Physics. 58, 845–852 (2017).
5. Gromyko Yu.V., Polivanov P.A., Sidorenko A.A., Bountin D.A., Maslov A.A., An experimental study of the natural noise in the Transit-M hypersonic wind tunnel. Thermophysics and Aeromechanics. 20, 481-493 (2013).
6. W. Cook and E. Felderman. Reduction of data from thin film heat transfer gauges: a concise numerical technique. AIAA J., 4, 561-562 (1966).
7. E. R. Van Driest and W. D. McCauley, The Effect of Controlled Three-Dimensional Roughness on Boundary-Layer Transition at Supersonic Speeds. J. Aeronaut. Sci. 27, 261-271 (1960).
8. M. C. Wilder, D. C. Reda, and D. K. Prabhu, Effects of Distributed Surface Roughness on Turbulent Heat Transfer Augmentation Measured in Hypersonic Free Flight. AIAA Paper No. 2014-0512 (2014).